

RESEARCH

Open Access



Synthesis and biological evaluation of [^{131}I]iodocarvedilol as a potential radiopharmaceutical for heart imaging

M. A. Motaleb^{1*}, K M Attalah¹, H A Shweeta¹ and I. T. Ibrahim¹

Abstract

The optimization of the radiolabeling yield of carvedilol with iodine-131 was described. Dependence of the labeling yield of [^{131}I]iodocarvedilol on the concentration of carvedilol, chloramine-T content, pH of the reaction mixture and reaction time was studied in details. Carvedilol was labeled with iodine-131 at pH 6 with a labeling yield of $92.6 \pm 2.77\%$ by using 100 μg carvedilol, 200 μg chloramin-T (CAT) and 30 min reaction time. The formed [^{131}I]iodocarvedilol was nearly stable for a time up to one day. Biodistribution of [^{131}I]iodocarvedilol was investigated in experimental animals. [$^{131/123}\text{I}$]iodocarvedilol was located in the heart with a concentration of $19.6 \pm 0.41\%$ of the injected dose at 60 min post injection. It has a high heart uptake and heart to liver ratio, both of which are beneficial for high-quality SPECT (single-photon emission computerized tomography) myocardial imaging. [$^{131/123}\text{I}$]iodocarvedilol solve most the drawbacks of the FDA (Food and Drug Administration) approved $^{99\text{m}}\text{Tc}$ -sestamibi.

Keywords Carvedilol, Imaging, Iodine-131, Labelling, Heart

Introduction

A blockage of the arteries that supply the heart muscle is known as coronary artery disease (CAD). Chest aches and breathing difficulty are signs of partial blockage, which results in lower blood supply to the heart. A complete obstruction of these veins can cause myocardial infarction by weakening and/or killing portions of the heart tissue caused by a lack of oxygen. The most common kind of heart disease and the major cause of death worldwide for both men and women is coronary artery disease (CAD).

Myocardial perfusion imaging (MPI) is a non-invasive imaging technology that utilizes an intravenously administered radiopharmaceutical to determine the distribution of blood flow in the myocardium during both rest and stress [1, 2].

The radiopharmaceutical must first reach the myocardium, where it must be up taken by live cardiac cells [3, 4].

Myocardial uptake directly relates to flow of blood, high extraction fraction, high target-to-background (T/B) ratio, good myocardial persistence (exhibiting sustained holding in the myocardium) and photon flux [5] where all of the above are desirable ideal features of a perfusion radiopharmaceutical [6].

Thallium-201 (^{201}Tl) and $^{99\text{m}}\text{Tc}$ -based myocardial perfusion tracers are used in SPECT.

The sodium-potassium adenosine triphosphatase (Na/K-ATPase) pump is responsible for ^{201}Tl extraction

*Correspondence:

M. A. Motaleb
mamotaleb10@yahoo.com

¹Labeled Compounds Department, Hot Laboratories Centre, Egyptian Atomic Energy Authority (EAEA), 13759 Cairo, Egypt



© The Author(s) 2023. **Open Access** This article is licensed under a Creative Commons Attribution 4.0 International License, which permits use, sharing, adaptation, distribution and reproduction in any medium or format, as long as you give appropriate credit to the original author(s) and the source, provide a link to the Creative Commons licence, and indicate if changes were made. The images or other third party material in this article are included in the article's Creative Commons licence, unless indicated otherwise in a credit line to the material. If material is not included in the article's Creative Commons licence and your intended use is not permitted by statutory regulation or exceeds the permitted use, you will need to obtain permission directly from the copyright holder. To view a copy of this licence, visit <http://creativecommons.org/licenses/by/4.0/>. The Creative Commons Public Domain Dedication waiver (<http://creativecommons.org/publicdomain/zero/1.0/>) applies to the data made available in this article, unless otherwise stated in a credit line to the data.

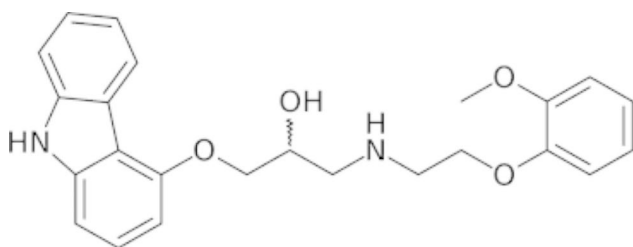


Fig. 1 Chemical structure of carvedilol

in the heart, hence its extraction fraction is influenced by both ATPase function and blood flow [7]. Thallium-201 has a physical half-life of 73 h and emits x-rays with energies of 67–82 KeV and gamma rays with energies of 135–167 KeV.

The picture quality of thallium-201 is worse than that of technetium-labeled agents [8–10], which has limited its application [11].

^{99m}Tc -Sestamibi, ^{99m}Tc -tetrofosmin and ^{99m}Tc -teboroxime have been approved by the FDA [12]. They all passively traverse cell membranes and have distinct myocardial accumulation and clearance characteristics. Despite having poor extraction and biodistribution qualities, due to their higher energy photons and low redistribution profiles, all three offer images of higher quality than ^{201}Tl .

In nuclear cardiology, ^{99m}Tc -Sestamibi has been frequently utilized for MPI. Owing to its high liver uptake [13] and roll-off at greater blood flow levels, it does not match the criteria of an ideal perfusion imaging tracer.

The high liver uptake makes evaluating cardiac activity in the inferior and left ventricular walls difficult [14].

Photon scattering from significant liver activity remains a major obstacle for successful SPECT diagnosis of heart dysfunction, despite ongoing attempts to eliminate this interference.

As a result, developing a novel perfusion radiopharmaceutical with superior biodistribution and/or extraction capabilities would be extremely beneficial [15–17].

Carvedilol is an antihypertensive drug that is used to treat elevated blood pressure and heart failure. It's also used to boost your chances of survival after a heart attack if heart isn't working well. Carvedilol binds to β -adrenergic receptors on cardiac myocytes in a reversible manner.

The inhibition of these receptors inhibits the sympathetic nervous system from responding, resulting in a drop-in heart rate and contractility. This action is beneficial in heart failure patients [18] where the sympathetic nervous system is activated as a compensatory mechanism (Fig. 1) [19].

The aim of the present work was to establish a simple and efficient method for radiosynthesis, characterization and biological evaluation of [^{131}I]iodocarvedilol

as a potential myocardial perfusion imaging radiopharmaceutical.

Experimental

Carvedilol was purchased from Memphis pharmaceutical company; Egypt and all other chemicals were purchased from Merck and they were analytical reagents.

Labeling procedure

Under oxidative circumstances in the presence of CAT, [^{131}I]iodocarvedilol was frequently produced via direct electrophilic substitution with no carrier added (NCA) ^{131}I . NCA ^{131}I allows for the use of high specific activity iodide without the need for carrier iodine.

The effect of different reaction parameters and conditions on radiolabeling efficiency, like the amount of oxidizing agents (CAT), carvedilol concentration [10 to 300 μg , (2.46×10^{-5} to 7.38×10^{-4} mM)], reaction pH (3–10), and reaction time (5–120 min), were studied and optimized in order to maximize radioiodination yield. No-carrier-added Na^{131}I (7.2 MBq) was transferred to the reaction flask. A freshly generated CAT in methanol was added to the reaction mixture, followed by 100 μg (2.46×10^{-4} mM) of carvedilol in methanol. For 15 min, the reaction mixture was agitated using a magnetic stirrer at room temperature. A drop of 10% saturated sodium thiosulfate (10 mg/mL in H_2O) was added to breakdown the excess iodine (I_2) and stop the reaction by reducing it to iodide (I^-) as it oxidizes to tetrathionate ($\text{S}_4\text{O}_6^{2-}$) [20], [21].

The radioiodinated product was separated, and TLC (Thin Layer Chromatography) was used to determine the radioiodination yield and purity of the product.

Analysis

Thin-layer chromatography was used to determine the radiochemical yield and purity [22] of [^{131}I]iodocarvedilol utilizing strips of silica gel coated on an alumina sheet.

1–2 μL of the reaction mixture was put 3 cm above the lower edge of a TLC strip (1.5 cm width, 15 cm length) and allowed to evaporate gradually.

HPLC (High-performance liquid chromatography) analysis: The radiochemical yield of [^{131}I]iodocarvedilol was calculated by injecting 10 μL of the reaction mixture into the column Rp-18 (250 mm x 4.6 mm, 5 μm) constructed in the HPLC (Shimadzu model), which contains a set of pumps LC-9 A, Rheohydrion injector (Syringe Loading Sample Injector-7125), and UV spectrophotometer detector (SPD-6 A). A mixture of acetonitrile/water (65:35) containing 0.1% trifluoroacetic acid was used as mobile phase, at a flow rate of 1.0 mL/min. The labeled compound was collected separately by using a fraction collector up to 12 min and its activity was counted by

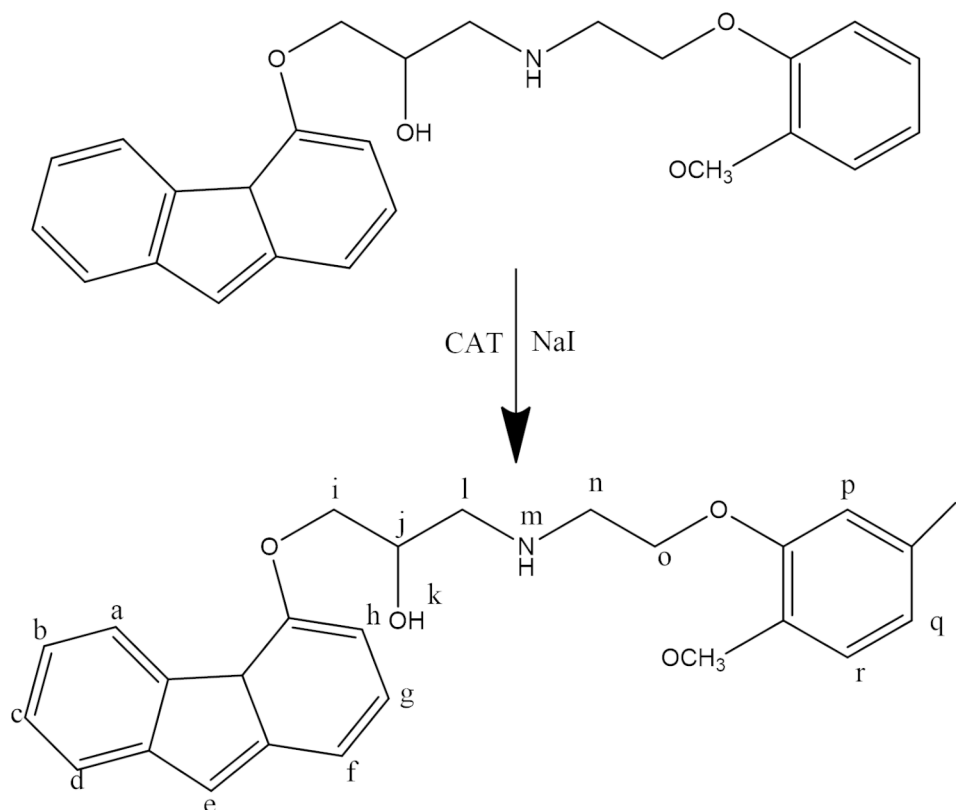


Fig. 2 Suggested structure of ^{127}I -carvedilol

using well a type NaI(Tl) crystal connected to a single-channel analyzer.

Nonradioactive iodination of carvedilol

Carvedilol was labeled with non-radioactive iodine with the chloramine-T method. Iodination of carvedilol generally follows the same chemistry used for radioactive iodination. Carvedilol (100 mg) was dissolved in minimum amount of methanol then a mixture of 200 μg chloramine-T and 15 mg NaI solution was added with vigorously stirring over 60 min for 1.5 h. The reaction products were separated with high performance liquid chromatography. The $^1\text{H-NMR}$ of ^{127}I -iodocarvedilol is similar to that of the carvedilol itself except the hydrogen in the para position to OCH_3 phenyl side chain which is different. $^1\text{H-NMR}$ (δ ppm):

8.2 (d, 1 H, a indole ring CH), 7.1 (d, 1 H, b indole ring CH), 7.11 (t, 1 H, c indole ring CH), 7.25 (d, 1 H, d indole ring CH), 11.2 (s, 1 H, e indole ring NH), 6.7 (d, 1 H, f indole ring CH), 7.3 (t, 1 H, g indole ring CH), 7.45 (d, 1 H, h indole ring CH), 4.15 (m, 3 H, i, j 2 *H*-methylene CH_2 and 1 *H*-methine CH), 5.2 (d, 1 H, k alcohol OH), 2.8 (m, 2 H, l methylene CH_2), 2.1 (s, 1 H, m amine NH), 2.9 (t, 2 H, n methylene CH_2), 4 (t, 2 H, o methylene CH_2), 6.9 (s, 1 H, p 1-benzene ring), 6.8 (m, 2 H, q, r 1-benzene ring) and 3.7 (s, 3 H, t CH_3) as shown in Fig. 2.

In vitro stability of ^{131}I iodocarvedilol

In vitro, the stability of ^{131}I iodocarvedilol was investigated by combining 1 ml normal serum with 0.5 mL ^{131}I iodocarvedilol and incubating for 24 h at 37 $^\circ\text{C}$.

During the incubation, 0.2 mL aliquots were taken at varied time intervals up to 24 h and exposed to TLC to determine the percent of ^{131}I iodocarvedilol and free iodine.

As a result, the radiolabeled compound stability will decide its potential for in vivo application.

Determination of octanol-water partition coefficient (log po/w)

Log P values of ^{131}I iodocarvedilol was determined using the following procedure: the ^{131}I iodocarvedilol was prepared and purified by HPLC. The collected mobile phases were evaporated and the residue was dissolved in a mixture of equal volume (3 mL:3 mL) *n*-octanol and water. After vortex for >20 min, the mixture was centrifuged at 8,000 rpm for 5 min. Samples (in triplets) from aqueous and *n*-octanol were obtained and counted separately in a gamma counter. The partition coefficients were calculated using the equation: $P = (\text{activity concentration in } n\text{-octanol}) / (\text{activity concentration in water})$. The log P value was measured three different times and reported

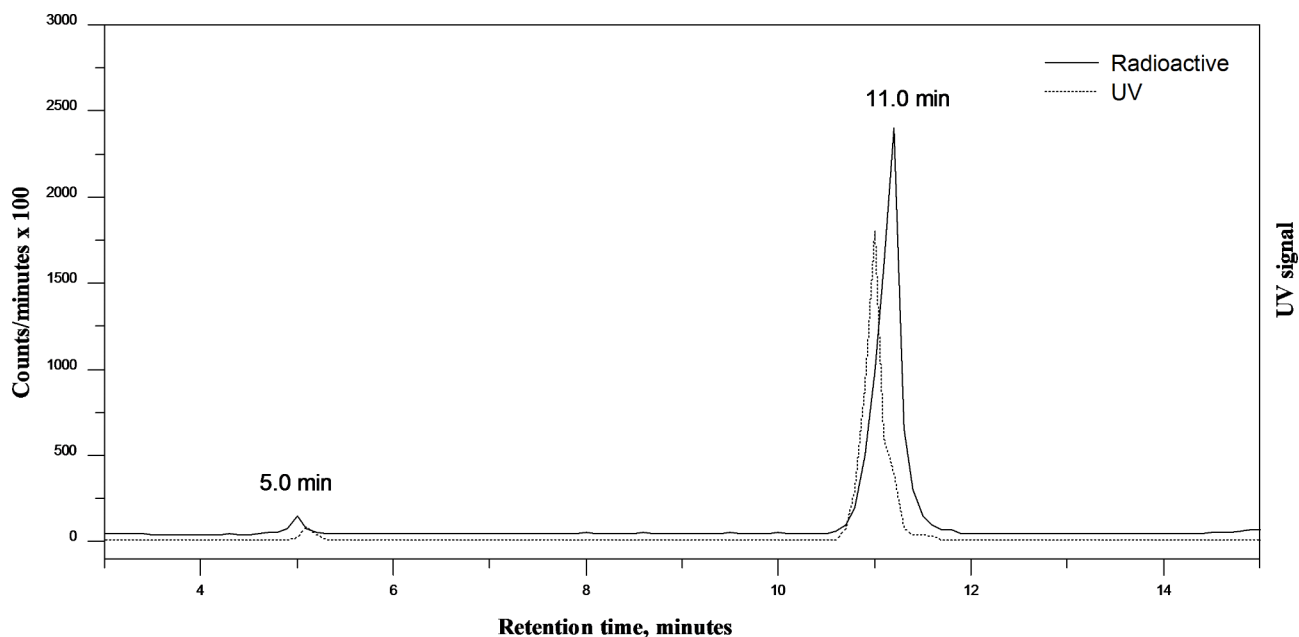


Fig. 3 HPLC chromatogram for [¹³¹I]iodocarvedilol

as an average of three different measurements. The calculated lipophilicity equal to 1.8.

Biological evaluation

The animal experimental protocols followed the Egyptian Atomic Energy Authority's rules and were approved by the animal ethics committee of the Labeled Compound Department. The biodistribution of [¹³¹I]iodocarvedilol was studied in normal rats (purchased from Egyptian National Research Center) (n=5) after 0.5, 1, and 3 h post injection (pi). Animals were housed in groups of five and given food and water prior to the study. Each animal received an aliquot of 10 μ L containing 3.7 MBq of the purified [¹³¹I]iodocarvedilol via the tail vein. Each animal was housed separately before being sacrificed by cervical dislocation at 0.5, 1, and 3 h following [¹³¹I]iodocarvedilol injection (n=5). Following sacrifice, each rat was weighed, and blood was collected from the heart and weighed. Muscles, bone, and blood were predicted to contribute for 40, 10, and 7% of total body weight, respectively [23]. Organs and tissues were cleaned with saline, collected in plastic containers, and weighed after dissection. In a well type NaI(Tl) well crystal linked to an SR-7 scaler ratemeter [24], the radioactivity of each sample as well as the background was quantified. For each time point, the percent injected dose (ID) per organ (percent ID/organ S.D.) in a population of five rats is presented. The Student t test was used to assess data differences. The two-tailed test results for *p* are presented, and all results are given as mean \pm SEM. The level of significance was set at *p* \leq 0.05.

Results and discussion

TLC was used to determine the radiochemical purity of [¹³¹I]iodocarvedilol, with a developing solvent mixture of methylene chloride: ethyl acetate (2:1 v/v), where radioiodide (¹³¹I) remained near the origin ($R_f = 0-0.5$), while [¹³¹I]iodocarvedilol moved with the solvent front ($R_f = 0.7-1$). The percentage radioiodination yield was calculated as the ratio of the radioactivity of [¹³¹I]iodocarvedilol to the overall activity, The average of three tests is used to calculate the radioiodination yield of [¹³¹I]iodocarvedilol. The radiochemical purity was further confirmed by HPLC analysis, where the retention time of free iodide and [¹³¹I]iodocarvedilol were 5 and 11 min, respectively, as shown in the chromatogram (Fig. 3). The UV chromatogram shows a peak at 10.9, which corresponds to cold iodocarvedilol, which coincides with the [¹³¹I]iodocarvedilol that appeared nearly at the same retention time in the radio-chromatogram.

Effect of reaction time

The yield of labelling is highly influenced by reaction time, which might range from 5 to 120 min. Figure 4 shows that increasing the reaction time from 5 to 30 min increases the yield significantly. The radiochemical yield is unaffected by increasing the reaction time beyond 30 min. The maximal radiochemical yield ($92.6 \pm 2.77\%$) requires a minimum reaction time of 30 min.

Effect of carvedilol amount

Figure 5 shows the relationship between radiochemical yield and carvedilol amount, where the radiochemical yield increased from 82.3 to 92.6% as the amount

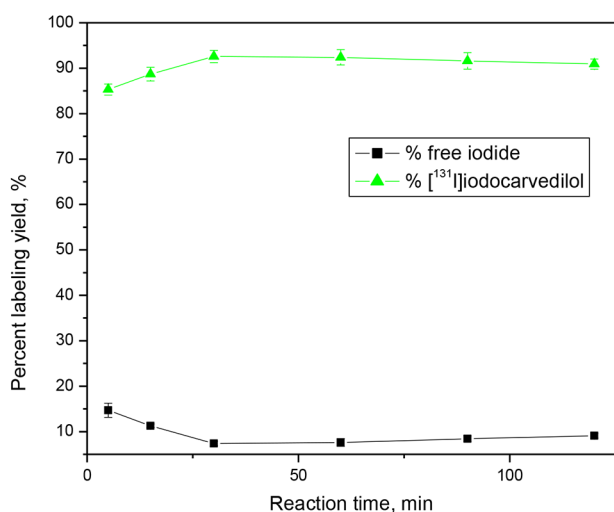


Fig. 4 Effect of Reaction time on the radiochemical yield of $[^{131}\text{I}]$ iodocarvedilol. Reaction conditions: 100 (2.46×10^{-4} mM) μg carvedilol (50 μl) + 200 μg (8.79×10^{-4} mM) CAT (20 μl) + 10 μl Na^{131}I for $\frac{1}{2}$ hour at pH 6 and 25 $^{\circ}\text{C}$; n=3

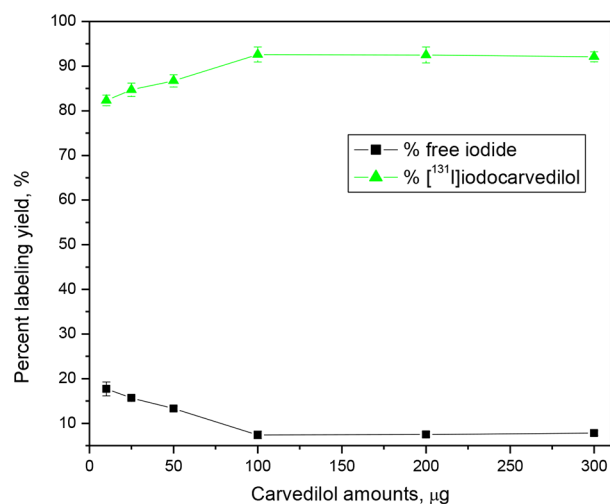


Fig. 5 Effect of substrate amount on the radiochemical yield of $[^{131}\text{I}]$ iodocarvedilol. Reaction conditions: X μg substrate + 200 μg

of carvedilol rose from 10 to 300 μg (2.46×10^{-5} to 7.38×10^{-4} mM). Further increases in the amount of carvedilol beyond 100 mg had no effect on the labelling yield, which might be explained by the fact that this concentration of carvedilol (100 μg , 2.46×10^{-4} mM) is sufficient to capture the full produced iodonium ion, resulting in the highest yield ($92.6 \pm 2.7\%$).

Effect of CAT concentration

After increasing the amount of CAT from 10 to 300 μg (4.39×10^{-5} to 1.3×10^{-3} mM) at pH 6 and a 30 minute reaction time, a high radiochemical yield ($92.6 \pm 2.7\%$) was obtained. The formation of undesired oxidative

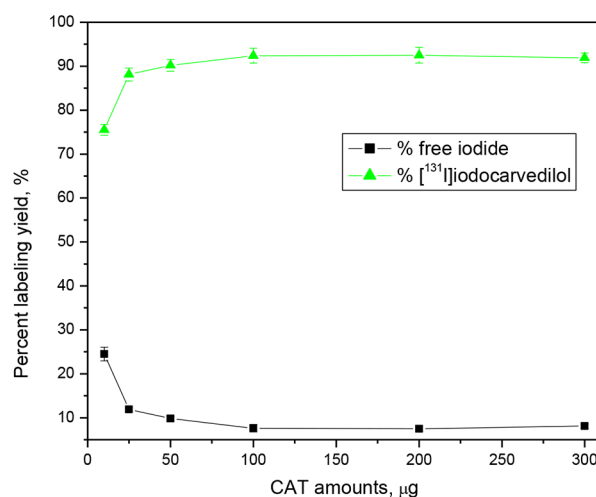


Fig. 6 Effect of CAT content on the radiochemical yield of $[^{131}\text{I}]$ iodocarvedilol. Reaction conditions: 100 μg (2.46×10^{-4} mM) sub-

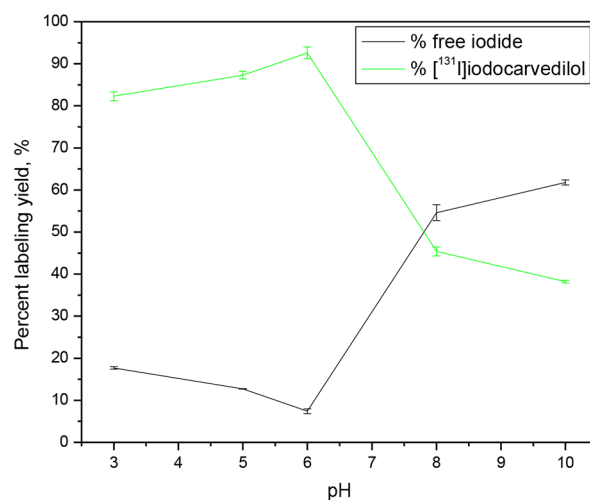


Fig. 7 Effect of pH on the radiochemical yield of $[^{131}\text{I}]$ iodocarvedilol. Reaction conditions: 100 μg (2.46×10^{-4} mM) carvedilol (50 μl) + 200 μg (8.79×10^{-4} mM) CAT (20 μl) + 10 μl Na^{131}I for $\frac{1}{2}$ hour at different pH, at 25 $^{\circ}\text{C}$; n=3

by-products such chlorination, polymerization, and denaturation of Carvedilol causes a drop in iodination yield when the CAT concentration is increased over 200 μg (8.79×10^{-4} mM) [25]. The high reactivity and concentration of CAT [2] may be responsible for the production of these contaminants. As a result, the optimal concentration of CAT is strongly advised in order to avoid the occurrence of by-products and achieve high yield and purity (Fig. 6).

Effect of pH of the reaction mixture

Figure 7 shows the effect of the reaction mixture pH on the radioiodination yield of $[^{131}\text{I}]$ iodocarvedilol. The

Table 1 *In-vitro* stability of [¹³¹I]iodocarvedilol

Time/hour	% Labeled compound	% Free iodide
1	92.6 ± 0.36	7.4 ± 0.1
2	91.4 ± 0.5	8.6 ± 0.15
4	88.1 ± 0.3	11.9 ± 0.2
24	86.2 ± 0.4	13.8 ± 0.1

Values represent the mean ± SEM n=6

reaction medium's pH was measured in the range of 3 to 10.

The redox potential of chloramine-T is pH dependent and decreases as the medium's pH rises [26], implying that the type of active oxidizing species of CAT is influenced by the medium's pH and reaction conditions. When chloramine-T is dissolved in water, it breaks down to ArSO₂NCl, which is hydrolyzed in an acidic medium to produce HOCl. The hypochlorous acid is hydrolyzed further to produce H₂OCl⁺.

HOCl and H₂OCl⁺ are probable oxidizing species in acidified CAT solutions, while HOCl and ClO are possible oxidizing species in alkaline CAT solutions.

Under acidic circumstances, the produced HOCl or H₂OCl⁺ oxidized the iodine to the oxidative state I⁺ (iodonium) [27], which quickly reacts with any sites within carvedilol that can undergo electrophilic substitution reactions [26, 28, 29]. Due to the maximal action of CAT at almost neutral pH, the remarkable stability of the carvedilol structure, and the good protonation of the aromatic ring at this pH value, the yield was maximized (92.6 ± 2.77%), yielding H⁺, which was substituted by the active iodonium ion I⁺. The yield dropped dramatically when the pH of the reaction medium was changed to the high acidic side, reaching 82.3% at pH 3. Also, the yield was quite low on the alkaline side, reaching 45.4 and 38.3% at pH 8 and 10, respectively. The synthesis of hypoiodite ion (IO⁻) and iodate (IO₃⁻) [30], which are not appropriate forms for radioiodination of carvedilol, could explain the decrease in radiochemical yield at alkaline pH.

Stability test

Due to the decomposition of the [¹³¹I]iodocarvedilol, incubation of the preparation containing [¹³¹I]iodocarvedilol for 24 hours at 37 °C resulted in a small decrease in the yield of [¹³¹I]iodocarvedilol (92.6 ± 2.77%) and the release of radioactivity from the [¹³¹I]iodocarvedilol was 5.9 ± 1.1%, as determined by ITLC (Table 1).

In-vivo studies of [¹³¹I]iodocarvedilol

In compliance with the guidelines set out by the Egyptian Atomic Energy Authority, the animal Ethics Committee, Labeled Compounds Department, and the protocol approval of Research Ethics Committee in the Faculty of

Table 2 Biodistribution of [¹³¹I]iodocarvedilol in normal rats

Organs & Body fluids	% Injected dose/gram tissue at different time intervals, min			
	15	30	60	120
Blood	1.47 ± 0.13	0.21 ± 0.05	0.15 ± 0.02	0.20 ± 0.03
Bone	2.55 ± 0.17	1.43 ± 0.35	1.01 ± 0.21	0.8 ± 0.01
Muscle	4.17 ± 0.79	1.5 ± 0.04	1.2 ± 0.1	0.5 ± 0.02
Liver	12.74 ± 1.63	5.1 ± 0.15	2.5 ± 0.1	1.7 ± 0.1
Stomach	3.0 ± 0.03	2.6 ± 0.1	1.2 ± 0.16	1.1 ± 0.0
Intestine	6.4 ± 0.50	7.8 ± 0.3	8.8 ± 0.1	11.2 ± 0.03
Lung	5.5 ± 0.08	2.1 ± 0.12	1.3 ± 0.02	0.8 ± 0.01
Heart	24.5 ± 0.1	20.1 ± 0.3	19.6 ± 0.41	12.8 ± 0.25
Spleen	6.5 ± 0.31	2.9 ± 0.1	2.0 ± 0.02	1.7 ± 0.05
Kidney	30.2 ± 0.4	17.6 ± 0.6	10.6 ± 0.3	3.5 ± 0.06
Thyroid	1.1 ± 0.01	1.3 ± 0.01	1.2 ± 0.02	0.9 ± 0.05

Values represent mean ± SEM

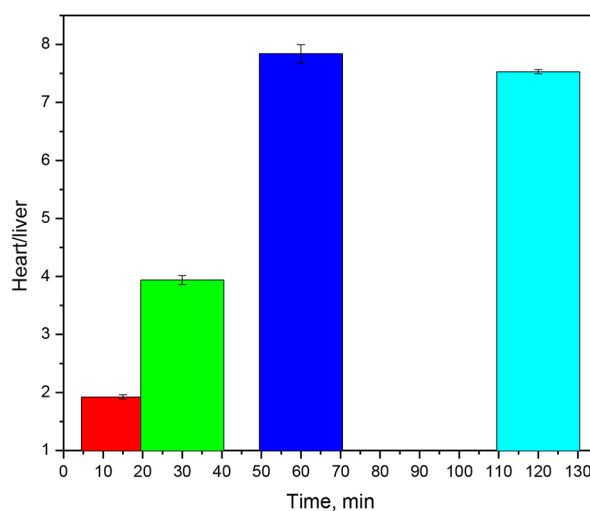


Fig. 8 The ratio of heart to liver uptake ratio of [¹³¹I]iodocarvedilol with time

Pharmacy, Cairo University (REC-FOPCU), Egypt, the biodistribution studies were performed.

Table 2 shows the results, which are expressed as percent dose per gram of tissue of [¹³¹I]iodocarvedilol. The biological distribution of [¹³¹I]iodocarvedilol in rats revealed that it had a great myocardial uptake, good heart persistence, and minimal uptake in the liver, lungs and blood. It was quickly removed from non-target tissues. Both kidneys and liver were the primary excretion organs pathway. The ratio of heart to liver uptake was high (1.922, 3.94, 7.84, 7.84 and 7.53 at 5-, 30-, 60- and 120-minute post-injection, respectively) (Fig. 8). The liver activity of [¹³¹I]iodocarvedilol was significantly decreased within the first hour compared with ^{99m}Tc-Sestamibi activity which declined more slowly over time.

The target-to-non-target ratios of ^{99m}Tc-sestamibi, a relatively successful myocardial imaging agent, are

Table 3 The ratios of target to non-target for [¹³¹I]iodocarvedilol and ^{99m}Tc-sestamibi in rats (n = 3)

Uptake ratio	[¹³¹ I]iodocarvedilol			^{99m} Tc-sestamibi		
	Post-injection time, min					
	5	30	60	5	30	60
Heart to liver	1.92	3.94	7.84	0.94	0.90	1.04
Heart to lung	4.46	9.57	15.1	2.87	9.07	12.25
Heart to blood	16.66	95.71	130.67	12.80	89.01	134.15

also presented in Table 3 [31] for comparison with [¹³¹I]iodocarvedilol.

[¹³¹I]iodocarvedilol had comparable heart to blood and heart to lung uptake ratios, but a significantly greater heart to liver uptake ratio, which is encouraging us to afford a novel myocardial imaging agent to get high-resolution scintigraphic images after using iodine-123 instead of iodine-131 (the same chemical properties).

Conclusion

In conclusion, using chloramine-T as an oxidizing agent, carvedilol was radiolabeled with NCA ¹³¹I by direct electrophilic substitution reaction with a high radiolabeling yield of 92.6 ± 2.77%. In rats, [¹³¹I]iodocarvedilol showed the right characteristics for use in cardiac imaging. It has a high heart uptake and heart to liver ratio, both of which are beneficial for high-quality SPECT myocardial imaging. [¹³¹I]iodocarvedilol solve most the drawbacks of the FDA approved ^{99m}Tc-sestamibi.

Abbreviations

CAD	Coronary artery disease
CAT	Chloramin-T
FDA	Food and Drug Administration
HPLC	High-performance liquid chromatography
ID	Injected dose
MPI	Myocardial perfusion imaging
Na/K-ATPase	Sodium-potassium adenosine triphosphatase
NCA	No-carrier-added
pi	Post injection
SPECT	Single-Photon Emission Computerized Tomography
T/B	Target-to-background ratio
TLC	Thin Layer Chromatography

Acknowledgements

Not applicable.

Author Contribution

MAM, KMA, HAS and ITI design the work and perform all experimental steps equally. All authors read and approved the final manuscript.

Funding

No funding.
Open access funding provided by The Science, Technology & Innovation Funding Authority (STDF) in cooperation with The Egyptian Knowledge Bank (EKB).

Data Availability

The datasets used and/or analyzed during the current study are available from the corresponding author on reasonable request.

Declarations

Ethics approval and consent to participate

In compliance with the guidelines set out by the Egyptian Atomic Energy Authority, the animal Ethics Committee, Labeled Compounds Department, and the protocol approval of Research Ethics Committee in the Faculty of Pharmacy, Cairo University (REC-FOPCU), Egypt, the biodistribution studies were performed. This study was conducted in accordance with the ARRIVE guidelines (<https://arriveguidelines.org>).

Consent for publication

Not applicable.

Competing interests

The authors declare that they have no competing interests.

Received: 26 August 2022 / Accepted: 3 March 2023

Published online: 15 March 2023

References

- Hung G-U. Diagnosing CAD: additional markers from myocardial perfusion SPECT. *J Biomedical Res.* 2013;27(6):467.
- Abd El-Karim SS, et al. Rational design and synthesis of new tetralin-sulfonamide derivatives as potent anti-diabetics and DPP-4 inhibitors: 2D & 3D QSAR, in vivo radiolabeling and bio distribution studies. *Bioorg Chem.* 2018;81:481–93.
- Beller GA, Zaret BL. Contributions of nuclear cardiology to diagnosis and prognosis of patients with coronary artery disease. *Circulation.* 2000;101(12):1465–78.
- Jain D. *Technetium-99m labeled myocardial perfusion imaging agents. In: Seminars in nuclear medicine.* Elsevier; 1999.
- Husain SS. Myocardial perfusion imaging protocols: is there an ideal protocol? *J Nucl Med Technol.* 2007;35(1):3–9.
- Bu L, et al. Evaluation of ^{99m}Tc-MPO as a new myocardial perfusion imaging agent in normal dogs and in an acute myocardial infarction canine model: comparison with ^{99m}Tc-sestamibi. *Mol imaging biology.* 2011;13(1):121–7.
- Carlin RD, Jan K-m. Mechanism of thallium extraction in pump perfused canine hearts. *J Nuclear Medicine: Official Publication Soc Nuclear Med.* 1985;26(2):165–9.
- Ziessman HA, O'Malley JP, Thrall JH. *Nuclear medicine: the requisites e-book.* Elsevier Health Sciences; 2013.
- Grunwald AM, et al. Myocardial thallium-201 kinetics in normal and ischemic myocardium. *Circulation.* 1981;64(3):610–8.
- Motaleb M, Moustapha M, Ibrahim I. Synthesis and biological evaluation of 125 I-nebivolol as a potential cardioselective agent for imaging β 1-adrenoceptors. *J Radioanal Nucl Chem.* 2011;289(1):239–45.
- Verberne HJ, et al. EANM procedural guidelines for radionuclide myocardial perfusion imaging with SPECT and SPECT/CT: 2015 revision. *Eur J Nucl Med Mol Imaging.* 2015;42(12):1929–40.
- Schwaiger M. Myocardial perfusion imaging with PET. *J Nucl Med.* 1994;35(4):693–8.
- Llaurado JG. The quest for the perfect myocardial perfusion indicator... still a long way to go. *J Nucl Med.* 2001;42(2):282–4.
- Kailasnath P, Sinusas AJ. Comparison of Tl-201 with Tc-99m-labeled myocardial perfusion agents: technical, physiologic, and clinical issues. *J Nuclear Cardiol.* 2001;8(4):482–98.

15. Banerjee S, Pillai MRA, Ramamoorthy N. *Evolution of Tc-99m in diagnostic radiopharmaceuticals*. In *Seminars in nuclear medicine*. Elsevier; 2001.
16. Liu S. *Ether and crown ether-containing cationic 99m Tc complexes useful as radiopharmaceuticals for heart imaging*. Dalton Transactions, 2007(12): p.1183–1193.
17. Sakr T, Moustapha M, Motaleb M. 99mTc-nebivolol as a novel heart imaging radiopharmaceutical for myocardial infarction assessment. *J Radioanal Nucl Chem*. 2013;295(2):1511–6.
18. Schwarz ER, et al. Carvedilol improves myocardial contractility compared with metoprolol in patients with chronic hibernating myocardium after revascularization. *J Cardiovasc Pharmacol Therap*. 2005;10(3):181–90.
19. Ozaydin M, et al. Nebivolol versus carvedilol or metoprolol in patients presenting with acute myocardial infarction complicated by left ventricular dysfunction. *Med Principles Pract*. 2016;25(4):316–22.
20. Motaleb M, et al. Radioiodinated paroxetine, a novel potential radiopharmaceutical for lung perfusion scan. *J Radioanal Nucl Chem*. 2012;292(2):629–35.
21. Rashed H, et al. Preparation of radioiodinated ritodrine as a potential agent for lung imaging. *J Radioanal Nucl Chem*. 2014;300(3):1227–33.
22. Selim AA, Motaleb M, Fayed HA. *Lung Cancer-Targeted [¹³¹I]-Iodoshikonin as Theranostic Agent: Radiolabeling, In Vivo Pharmacokinetics and Biodistribution* Pharmaceutical Chemistry Journal, 2022. 55(11): p. 1163–1168.
23. Motaleb M, et al. An easy and effective method for synthesis and radiolabeling of risedronate as a model for bone imaging. *J Label Compd Radiopharm*. 2016;59(4):157–63.
24. Ebrahim EM, et al. Histopathology, pharmacokinetics and estimation of interleukin-6 levels of Moringa oleifera leaves extract-functionalized selenium nanoparticles against rats induced hepatocellular carcinoma. *Cancer Nanotechnol*. 2022;13(1):1–26.
25. Motaleb M, et al. Novel radioiodinated sibutramine and fluoxetine as models for brain imaging. *J Radioanal Nucl Chem*. 2011;289(3):915–21.
26. Sukhdev A, Shubha J. Kinetics and reactivities of ruthenium (III)-and osmium (VIII)-catalyzed oxidation of ornidazole with chloramine-T in acid and alkaline media: a mechanistic approach. *J Mol Catal A: Chem*. 2009;310(1–2):24–33.
27. Selim AA, et al. Extraction, purification and radioiodination of Khellin as cancer theranostic agent. *Appl Radiat Isot*. 2021;178:109970.
28. Swamy P, Vaz N. Ruthenium (III)-and osmium (VIII)-catalyzed oxidation of 2-thiouracil by bromamine-B in acid and alkaline media: a kinetic and mechanistic study. *Transition Met Chem*. 2003;28(4):409–17.
29. Jagadeesh R. Os (VIII)-catalyzed and uncatalyzed oxidation of biotin by chloramine-T in alkaline medium: comparative mechanistic aspects and kinetic modeling. *J Mol Catal A: Chem*. 2007;265(1–2):70–9.
30. Ibrahim A, et al. Radioiodinated anastrozole and epirubicin as potential targeting radiopharmaceuticals for solid tumor imaging. *J Radioanal Nucl Chem*. 2015;303(1):967–75.
31. Chu J, et al. [^{99m}TcN (PNP5)(NOEt)]⁺: a novel potential myocardial perfusion imaging agent. *J Radioanal Nucl Chem*. 2006;269(1):175–9.

Publisher's Note

Springer Nature remains neutral with regard to jurisdictional claims in published maps and institutional affiliations.